Model Test on Base Mat Uplift of Nuclear Reactor Building
Part 2 : Field Tests on Actual Ground

Sadatomo ONIMARU, Tamio IMAZAWA
Takenaka Corporation, Tokyo, Japan
Yasuhiko HANGAI
University of Tokyo, Tokyo, Japan
Kinji AKINO
Nuclear Power Engineering Center (NUPEC), Tokyo, Japan

ABSTRACT

This paper describes the field tests planned to study the uplift phenomena of the reactor buildings. These tests were carried out at two actual ground sites which had different soil conditions. Static uplift tests and dynamic uplift tests were carried out. The results of these tests clarified the following : (1) When a base mat is uplifted, resonant frequency of model-ground system moves to the low frequency side. (2) The high frequency component appears in the response wave during uplift. (3) The characteristics obtained from these tests correspond well to those obtained by conventional design method.

1 INTRODUCTION

It has been predicted in view of the seismic design that the base mat uplift of rigid structures such as reactor buildings might occur during strong earthquakes. It is necessary to study the uplift phenomena of base mat from an innovative viewpoint through various experiments. Two kinds of tests, namely laboratory tests and field tests on actual ground, were carried out, and the adequacy of assumptions used in the current analytical methods was verified and basic data necessary to establish an appropriate response analysis method were also obtained. The results of the laboratory tests were presented at the 10th SMiRT Conference (Ref. 1).

This paper describes the results of the field tests on actual grounds.

2 OUTLINE OF TESTS

Static and dynamic uplift tests were conducted on actual grounds, and dynamic tests were conducted at two sites having different ground conditions.

The two sites (SITE1, SITE2) have hard rock which is suitable for the construction of a reactor building, but rock at SITE2 is softer than at SITE1. Soil properties at each site are presented in Table 1.

At SITE1, three test models were constructed for static and dynamic tests, and at SITE2, one model was constructed for dynamic uplift tests. These test models had the same shape shown in Fig. 1 and Table 2 , which was designed to make it easy to induce uplift in order to obtain clear uplift phenomena. They were blocks made of concrete and were regarded as rigid body. Small stress transducers were installed at the bottom of them in order to measure contact pressure distribution and contact ratio.

In the static uplift tests, force was applied by two hydraulic jacks with a

maximum capacity of 300tons installed between an existing large concrete block (reaction block) and the tops of the models (Fig. 2). The rotation angle, the displacement of the test models and the contact pressure were obtained from measuring instruments.

In the dynamic uplift tests, sinusoidal excitation was applied using an exciter installed on the top of the model (Fig. 3). The displacement, the acceleration of the test models and the contact pressure were obtained from each measuring instruments, and the rotation angle and the contact ratio was evaluated from them.

3 TEST RESULT

3.1 Static Uplift Test

The static relationship between the overturning moment and the rotation angle of the models is shown in Fig. 4. The symbols represent the result of the tests. The non-linearity is clearly shown by the uplift phenomena with an increase in the overturning moment. The solid line represents the result calculated by the conventional design method in which the distribution of contact pressure is assumed to be triangular(Ref. 1). The result of the tests correspond closely to the result obtained by the conventional design method.

Figure 5 shows the variation of the contact pressure distribution at the bottom of the model according as the load increases. The pressure values are normalized to be zero before horizontal loading. Figure 5 (a) represents the situation before uplift, and Figure 5 (b) represents the situation after uplift begins. Marks▼ indicate the positions where the tension side of contact pressure reaches the ceiling according as the load is added. These positions are where the uplift occurs. The progress of an uplift area can clearly be seen with an increase in the load. The contact ratio was estimated from this.

3.2 Dynamic Uplift Test

Basic dynamic characteristics of the test model-ground system, which were obtained from the resonance curves and phase lag curves when uplift did not occur, are presented in Table 3.

The dynamic characteristics of the test model-ground system changes once the uplift occurs. From the resonance curves of the displacement at the top of each model during uplift, the variation is confirmed (Fig. 6, Table 4). At each site, when exciting force increases, the contact ratio decreases, resonance frequency of the model-ground system shifts gradually to the low frequency side, and the gradient of the resonance curve suddenly rises at the resonance point.

The characteristics of the structure's response under the uplift can be seen from the response waveforms shown in Fig. 7 and Fourier spectra shown in Fig. 8. From these figures, flattened peaks and the occurrence of high frequency components are confirmed in the acceleration response wave. Particularly a component with triple frequency of the exciting frequency appears in the horizontal component and the double frequency component grows in the vertical component.

4 . EVALUATION OF TEST RESULTS

The following relationships are considered.

1) Relationship between overturning moment and rotation angle

The result of the static tests and that of the dynamic tests are represented in Fig. 9 with the curve calculated from the conventional design method. The dynamic overturning moment was determined from the exciting force and the acceleration of test models. From this figure, the results of the dynamic

uplift tests correspond well to that of the static uplift tests, and both the results of the tests approximately correspond to those obtained from the conventional design method.

2) Relationship between contact ratio and resonance frequency

Figure 10 shows the relationship between the contact ratio and the resonance frequency. It is confirmed that the resonance frequency shifts to the low frequency side according as the contact ratio decreases.

3) Relationship between contact ratio and overturning moment

As shown in Fig. 11, the contact ratio shows a tendency to decrease according as the overturning moment increases. And it is confirmed that the dynamic and static relationship obtained from the tests corresponded well to the results by the conventional design method (solid line). Also, it is verified that there is almost no difference between the results of static uplift tests and those of dynamic uplift tests.

5 CONCLUSION

The followings have been concluded from these results.

1) The more the exciting force increases, the more the contact ratio decreases with the progress of uplift, and resonance frequency of the test model- ground system moves to the low frequency side.

2) With the decrease of the contact ratio, components with even and odd number times frequency of the exciting frequency clearly appears in the acceleration response wave.

3) The relationship between the overturning moment and the rotation angle, and that between the overturning moment and the contact ratio correspond well to the results calculated from the conventional design method. In these relationships, the results of the static uplift tests also correspond well to those of the dynamic uplift tests.

4) Even if there are differences in the ground conditions, only the ground stiffness and the damping factor are different, and the characteristic phenomena and the relationship mentioned above show almost the same tendency.

These results of the field tests, which were carried out on actual ground, indicate a good correspondence to the results of the laboratory tests in characteristic behavior induced by an uplift which are described in Ref. 1

6 ACKNOWLEDGMENT

This work was carried out as the entrusted project sponsored by the Ministry of International Trade and Industry in Japan. This work was supported by "Sub-Committee of Base Mat Uplift" under "Committee of Seismic Verification Tests" of NUPEC.

The authors wish to express their gratitude for the co-operation and valuable suggestions given by the members of the Committee.

REFERENCES

1. Hangai, Y., Akino, K., et al., "Model Test of Base Mat Uplift of Reactor Building, Part1:Laboratory Test ", Vol. K1 pp. 169-174, 10th. Structural Mechanics in Reactor Technology, 1989.
2. Hangai, Y., Akino, K., et al., "Model Tests on Base Mat Uplift of Reactor Building, Part1 to Part6", Annual Meeting of Architectural Institute of Japan(AIJ), 1986(in Japanese).
3. Hangai, Y., Akino, K., et al., "Field Tests on Base Mat Uplift of Reactor Building, Part1 to Part6", Annual Meeting of AIJ, 1987(in Japanese).
4. Hangai, Y., Akino, K., et al., "Evaluation for Model Tests on Base Mat Uplift of Reactor Building, Part1 to Part7", Annual Meeting of AIJ, 1988(in Japanese).

Table 1 Soil profile

	Shear wave velocity	Density	Poisson's ratio	Young's modulus	Damping factor
SITE1	1050m/sec	2.1t/m³	0.39	6.56×10^{3}t/m²	4.0%
SITE2	930m/sec	2.0t/m³	0.40	4.96×10^{6}t/m²	5.0%

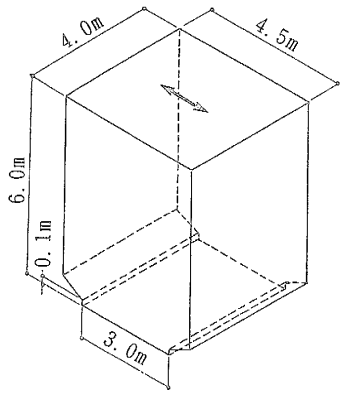

Fig. 1 Configuration of test model

Table 2 Properties of test model

Weight (including exciter)	261.6t
Rotation inertia (around the gravity center)	1251.3t·m²
Height of gravity center	3.141m
Height of loading point(static test)	5.6m
Height of exciting point(dynamic test)	6.4 m

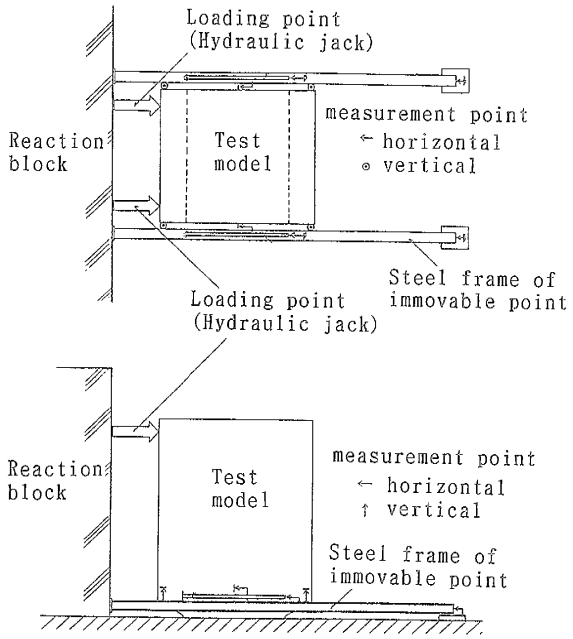

Fig. 2 Outline of static tests

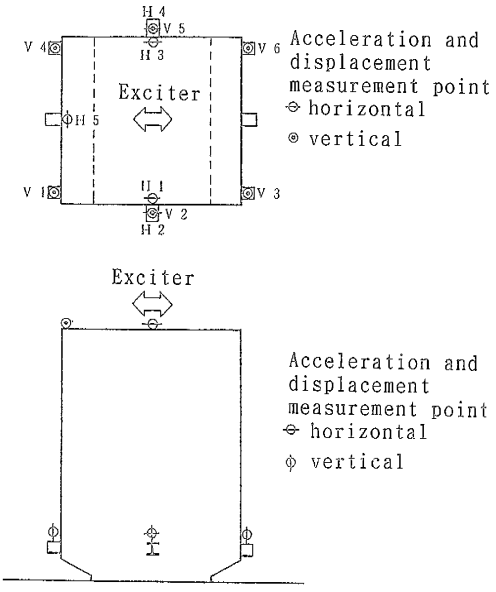

Fig. 3 Outline of dynamic tests

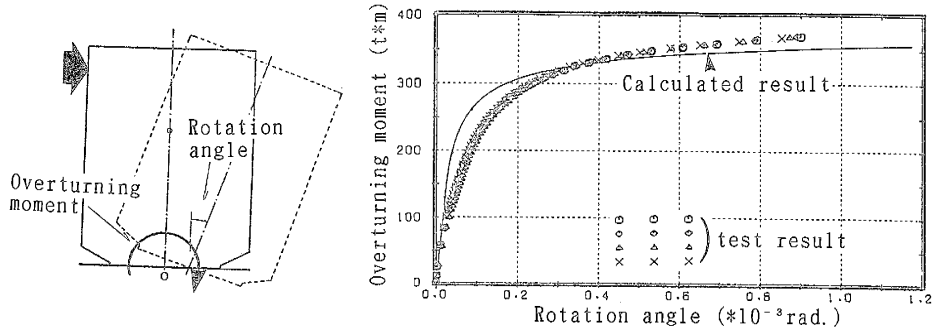

Fig. 4 Static relationship between overturning moment and rotation angle

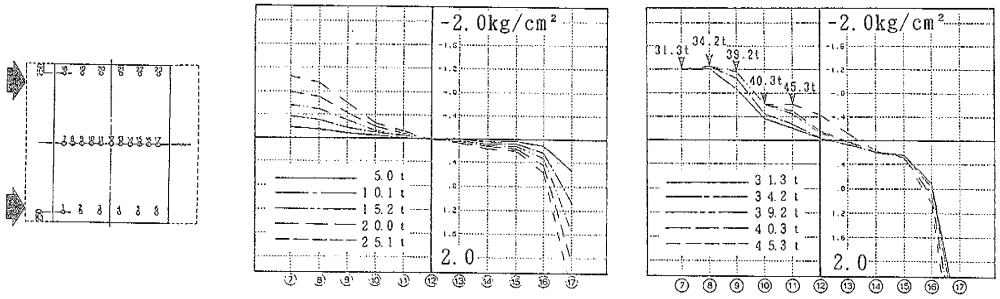

(a) Before uplift (b) After uplift

Fig. 5 Variation of the contact pressure distribution

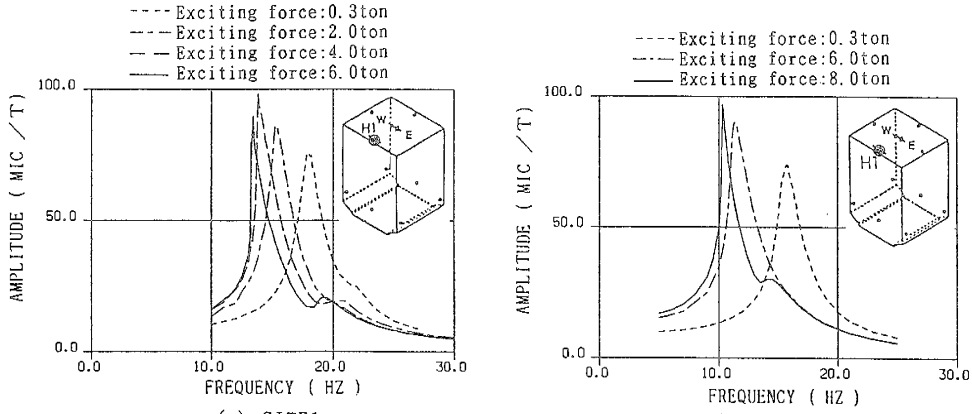

(a) SITE1 (b) SITE2

Fig. 6 Resonance curve of horizontal displacement at the top of model (Displacement is normalised by exciting force)

Table 3 Basic dynamic characteristics

	SITE1	SITE2
Resonance frequency: f_o(Hz)	18.0	15.7
Damping factor(%)	5.2	6.0

Table 4 Resonance frequency and contact ratio for exciting force

	SITE1				SITE2		
Exciting force (t)	0.3	2.0	4.0	6.0	0.3	6.0	8.0
Resonance frequency: f (Hz)	18.0	15.4	13.8	13.4	15.7	11.4	10.3
Contact ratio	1.0	0.8 ~ 0.9	0.7 ~ 0.8	0.4 ~ 0.5	1.0	0.8 ~ 0.9	0.6 ~ 0.7

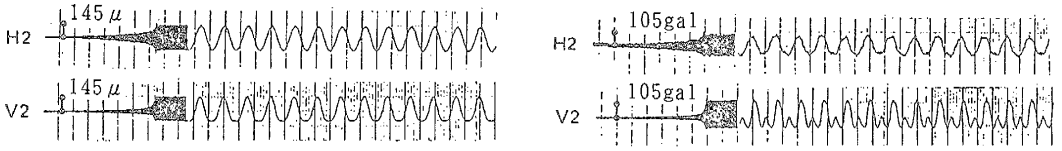

(a) Displacement (b) Acceleration

Fig. 7 Response waveform
(SITE2, Exciting frequency: 10.3Hz, Exciting force: 0～8ton)

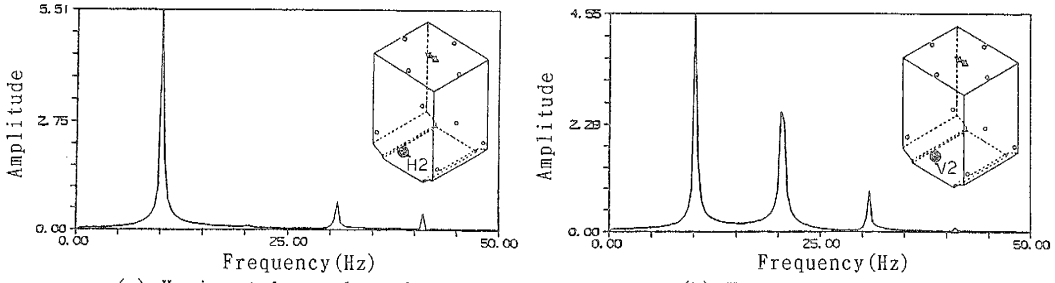

(a) Horizontal acceleration (b) Vertical acceleration

Fig. 8 Fourier Spectrum of response acceleration
(SITE2, Exciting frequency: 10.3Hz, Exciting force: 8ton)

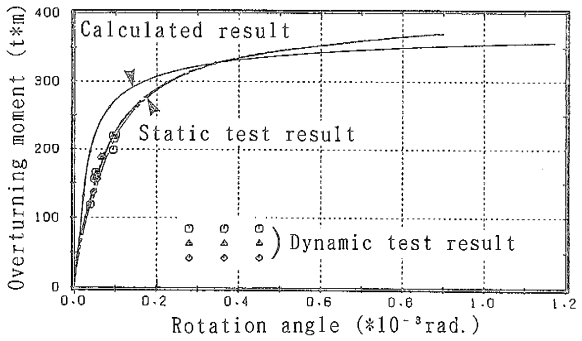

Fig. 9 Dynamic relationship between overturning moment and rotation angle

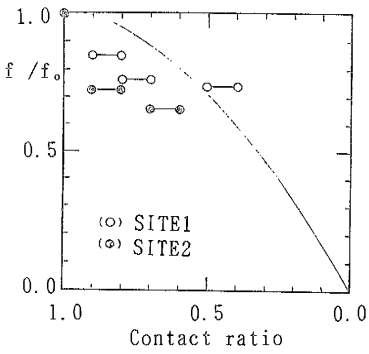

Fig. 10 Contact ratio and resonance frequency
(f₀:resonance frequency when uplift dosen't occur)

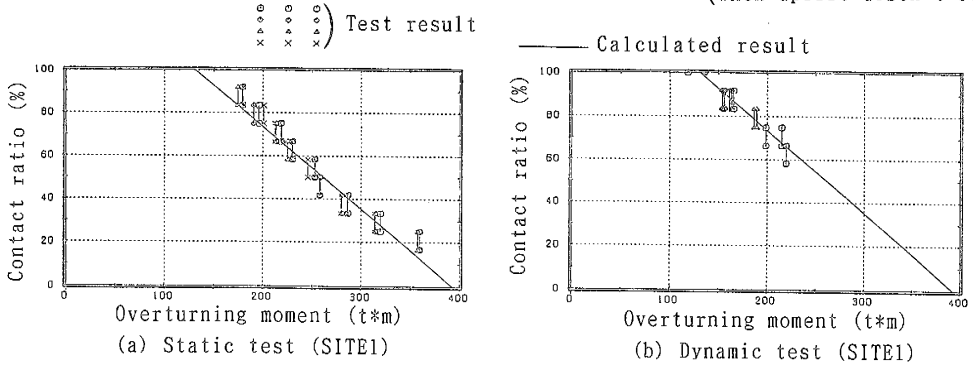

(a) Static test (SITE1) (b) Dynamic test (SITE1)

Fig. 11 Contact ratio and overturning moment